TOWARDS UNSTEADY APPROACH FOR FUTURE FLUTTER CALCULATIONS

Luc Mouton, Alban Leroyer, Ganbo Deng, P. Queutey, T. Soler, A. Finkelstein

TOWARDS UNSTEADY APPROACH FOR FUTURE FLUTTER CALCULATIONS

L. Mouton, Bureau Veritas, France, luc.mouton@bureauveritas.com
A. Leroyer, Centrale Nantes, LHEEA UMR-CNRS 6598, France, alban.leroyer@ec-nantes.fr
G.B. Deng , Centrale Nantes, LHEEA UMR-CNRS 6598, France, ganbo.deng@ec-nantes.fr
P. Queutey, Centrale Nantes, LHEEA UMR-CNRS 6598, France, patrick.queutey@ec-nantes.fr
T. Soler, Centrale Nantes, LHEEA UMR-CNRS 6598, France
A. Finkelstein, Farr Yacht Design, USA, alon@farrdesign.com

In prior work to define an improved hydrodynamic approach to flutter calculations, Centrale Nantes, Bureau Veritas Marine & Offshore and Farr Yacht design investigated the possibility of defining a linearized unsteady hydrodynamic model. The approach is compared to the Theodorsen theory. The linearized hydrodynamic model was used in a strip theory model for frequency domain flutter analysis.
In this latest work, the IMOCA 2006 keel which has been used previously in frequential domain flutter calculation is analysed using an alternative and more accurate solution, featuring a fully coupled FSI modal approach with CFD. Results are discussed.

NOMENCLATURE

ρ	Density of water (kg.m^{-3})
P_{dyn}	Dynamic pressure (N.m^{-2}), $1/2\rho V_\infty^2$
M, K	Mass, stiffness matrix
θ	Incidence of a foil section (rad)
h	Heave of the foil (m)
α_h	Heave apparent incident angle (rad) , $-\frac{\omega \dot{h}}{V_\infty}$
V_∞	Boat speed (m/s)
Re	Reynolds number
C	Mid chord point of the profile
O	Quarter chord point of the profile
B, b	Full chord, half chord (m)
X	Displacement vector characterizing the deformation of the keel (m; rad)
$\tilde{x}$	Variation of X around an equilibrium position
ω	Vibration of the motion (rad/s)
k	$\frac{\omega B}{V}$ reduced frequency
t_p, t_h	Delay of the pitch and heave motion compared to the time origin (m; rad)
L(t)	Lift force per unit of span (N/m)
M(t)	Pitch moment per unit of span (N/m)
L_0^{pitch}, L_0^{heave}	Lift amplitude induced by pitch and heave $\tilde{\theta}, \tilde{\alpha}_h$, (N/m)
$\varphi_0^{pitch}, \varphi_0^{heave}$	Lift phase of the lift induced by pitch and heave relative to the motion, (rad)
C_L	Lift coefficient
C_M	Pitch moment coefficient
FFT	Fast Fourier Transform

1. INTRODUCTION

At the 2015 HPYD conference, Burns Fallow from North Sails noted how quickly sailors become accustomed to extraordinary. Indeed four years ago, it was extremely rare for boats to actually 'fly'; only Hydroptere and a few foiling dinghies had this potential. After the 2013 America's Cup the number of fully foiling designs exploded. We are now witnessing the first fully foiling ocean going yachts. It is relevant to consider whether flutter will be an issue for larger and larger foils. Are foils not concerned by the hydro-structural instability, or is it simply that the design envelope is still below the dangerous area? And what is the margin between the actual designs and the flutter limit?
As a reminder, an unstable hydro-structural vibration or flutter caused the failure of the keel of the IMOCA 60 SILL in 2002. Since then several IMOCA 60's were subject to the phenomenon and which resulted in expensive and time consuming redesign efforts.
In 2015, the paper [1] presented the promising results of a modal hydro-structural flutter analysis. This approach used a very basic hydrodynamic model based on the heave and pitch motion of 2D hydrofoil strips. For structures such as keels, the model gave fairly accurate results and improved understanding of the phenomenon. The previously developed model can be used successfully to predict flutter in the sailing domain of a canting keel. For example this model can be used to produce optimized designs for yachts such as mini Transat 6.50 and maxis where the class rules do not require one design keels. In contrast other canting keel classes, like the VOR65 or the present IMOCA 60's have avoided flutter by requiring one-design boats and keels.
Unfortunately foils and keels are very different structures in terms of their dynamic response and the hydro-structural effect induced by lead carriers (keels) is very

different from the response observed on a high modal frequency foil. Hence, the first step was to study the difference between the two appendages and the available models in their response to unsteady flows.
The present paper relates the effort produced by the LHEEA lab and Bureau Veritas Marine & Offshore to enhance the flutter analysis possibilities from a quasi-static approach to an unsteady model. The first part of the work deals with the strip model of the hydro-structural modal calculation. The second part describes preliminary results using a fully coupled modal approach with CFD.

1.1 FLUTTER

The phenomenon of flutter is well known in the aviation industry. It was discovered at the beginning of the twentieth century on aircraft wings and was shown to be linked to a vibration problem. During flutter, a coupling of torsional and bending vibration modes of the structure and the aerodynamic forces leads to a transfer of energy from the fluid to the vibrating structure. This transfer of energy, even for a few seconds, can be enough to induce vibration amplitudes that can lead to complete failure of the wing structure. The phenomenon is said to be explosive.

1.2 LEAD BULBS AND FOILS, QUASI-STATIC AND UNSTEADINESS

The main objective of a keel is to carry a heavy lead bulb that will produce a large part of the overturning moment necessary to keep the boat upright under the massive force of the sails. If we consider a typical 2006 IMOCA keel design that experienced the onset of flutter, the bulb inertia lowers the natural frequencies of the keel to around:

- 1.0 Hz for the bending mode
- 2.15 Hz for the torsion mode

The appendage modal vibration creates a harmonic oscillation of the fin's section. A vibration of the torsional mode will see the fin section rotate a full oscillation in 0.46 sec. During this time, a particle of water travelling at 30 knots will travel a distance of 7.2 m. This means that after one oscillation, the particle has travelled 18 chord lengths downstream. In other words, the vortex wake induced by an oscillation of the profile will be very far aft of the profile at the end of one oscillation. As the influence of the vortex is inversely proportional to the distance, it will have a small impact on the profile. The hydrodynamic response can be considered quasi-static. This is characterised by a low reduced frequency k equal to 0.3 in this case.
On the other hand, a light and stiff foil will have natural frequencies on the order of 20 Hz. For the same chord and speed, a particle of water will travel only 1.1 chord lengths downstream during an oscillation. The vortex wake induced by the oscillation will exist directly downstream of the section of the foil at the end of the period. This proximity creates a potential influence of the vortex wake on the hydrodynamic forces of the next oscillation. The flow is said to be unsteady. The reduced frequency of this example is 5.3. Figure 1 illustrates this example.

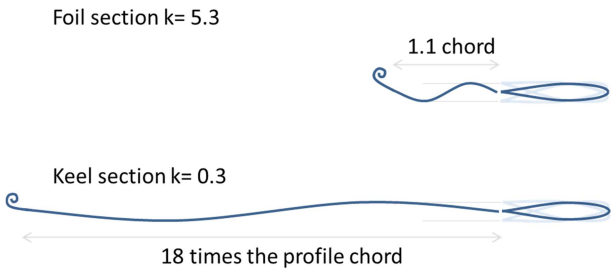

Figure 1: *Illustration of the reduced frequency and indication on the potential impact of the vortex induced sheet*

The number of chord lengths travelled by a particle of water (or a vortex wake) during a period of the oscillation is $2\pi/k$.

This explains why the quasi-static hydrodynamic model can give good results in the flutter calculation of a keel. However, to enable the faithful modelling of hydro-structural effect on a foil, it is necessary to take into account unsteady hydrodynamic effects.

Although it still needs validating, the unsteady effects are intrinsically considered in a URANSE code. However, the use of complex CFD tools for flutter evaluation is cumbersome as the creation of such a model is complex and time consuming. Therefore, the strip frequency domain model is remains interesting but it requires enhancement of its hydrodynamic models to consider high reduced frequency problems.

In order to better take into consideration the unsteady effects, two options are considered and compared. The first is the analytical Theodorsen model. This model considers a 2D wing section harmonically oscillating in a flow. As a function of the reduced frequency, it evaluates the lift amplitude and phase lag. Momentum can also be expressed, but not drag.

The second option is to build a 2D unsteady model representing a foil profile pitching or heaving in a steady state flow produced by CFD. By simulating the fluid forces produced by different sets of harmonic motion in a database, the latter can be used as input to the frequency domain tool in order to incorporate unsteady effects into the fluid model.

2. METHODOLOGY, MODELS AND TOOLS

The methodology is based on two tools: the first one, developed by Bureau Veritas takes its background from the aeronautical industry. It is based on the frequency domain analysis of a hydro-structure model. The second one, ISIS-CFD, is a Navier-Stokes solver developed at the LHEEA Lab., which is used here both to build a database as input to the previous tool and also to carry out a fully coupled time-marching resolution of this fluid-structure interaction problem.

2.1 MODAL HYDRO-STRUCTURAL FLUTTER ANALYSIS

The structural model is based on a truncated series of the *n* most energetic modes, without limitation on the number of modes. Accounting for two modes in a keel analysis is sufficient, but would be insufficient to analyse properly light structures such as a hydrofoil. The inputs to the flutter analysis software are the dry mode natural frequencies, shapes (normalized using the diagonalized mass matrix) provided as an output from Finite Element Analysis (FEA) of the structure.

Laws of dynamics give the following equation for the dry system with or without heel:

$$M\ddot{X} + KX = F_{Gravity} \qquad (1)$$

As a reminder, and as detailed in [1], the strip model consists of several slices the fin profile along the span. During any vibration of the keel or foil, the motion of each slice can be described with 6 degrees of freedom among which two are identified as having an impact on the hydrodynamic flow.

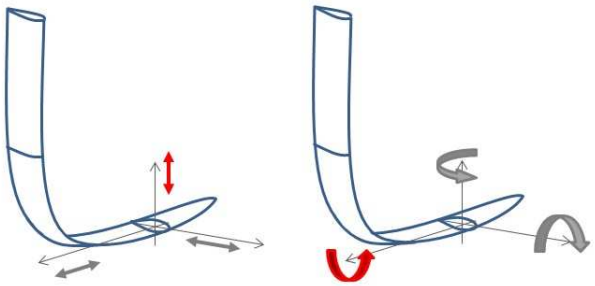

Figure 2 *Foil section with three possible translation (left) and three possible rotation (right). Motions with significant impact on the hydrodynamic are plotted in red*

In the local axis of a fin section (span wise, chord wise and perpendicular to the mean plane) the motion of the section profile can be named heave and pitch as described in figure 3. The hydrodynamic loads in the respective direction are the drag, lift and pitching moment. For the sake of simplicity, only the lift will be shown here, but it should be noted that what follows can be reproduced for the other hydrodynamic loads.

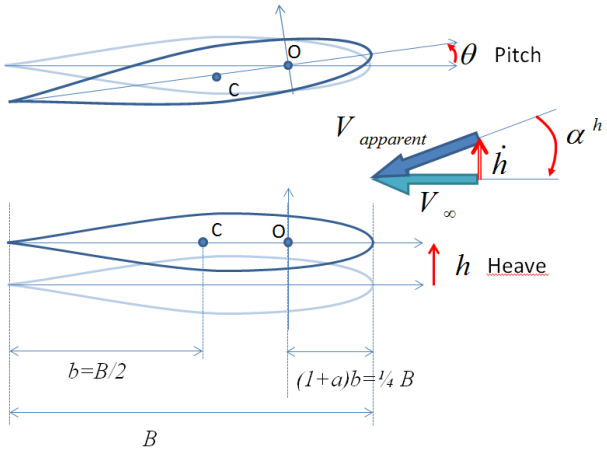

Figure 3 *Section profile motions in the reference axes of the undeformed foil*

It is important to differentiate two separate concepts: modes and motions. A mode is a natural response of a structure with a natural frequency and shape which comes from a linearized reduced model of the structure. Therefore, any structural mode can be understood at the level of a section profile (or slice), as a combination of 6 degrees of freedom. Among these, 2 are in our focus because of their hydrodynamic impact: pitch and heave (see figure 3).

2.1.1 2D FLAT FOIL SECTION HARMONICALLY OSCILLATING IN PITCH AND HEAVE

Let's consider a 2D profile section oscillating of small variations $\tilde{x}$ around an equilibrium position X_0 :

$$X = X_0 + \tilde{x} \qquad (2)$$

If we consider harmonic motions around the equilibrium position, the motion can be written as:

$$\tilde{x}(t) = \begin{bmatrix} \tilde{\theta}(t) = \Re e(\theta_0 e^{i\omega(t-t_p)}) \\ \tilde{h}(t) = \Re e(h_0 e^{i\omega(t-t_h)}) \end{bmatrix} \qquad (3)$$

Assuming the uncoupled hydrodynamic response we can write the unsteady lift per unit span:

$$\tilde{L} = \tilde{L}^{pitch}(\tilde{\theta}, \dot{\tilde{\theta}}, \ddot{\tilde{\theta}}) + \tilde{L}^{heave}(\dot{\tilde{h}}, \ddot{\tilde{h}}) \qquad (4)$$

In the hypothesis of small motions around the equilibrium position, we make the assumption that the hydrodynamic response is harmonic and its spectral content is purely in the first harmonic of the initial motion:

$$\tilde{L} = L_0^{pitch}.e^{i\varphi_L^p}.e^{i\omega(t-t_p)} + L_0^{heave}.e^{i\varphi_L^h}.e^{i\omega(t-t_h)} \qquad (5)$$

where $L_0^{pitch}; L_0^{heave}; \varphi_L^p; \varphi_L^h$ are real numbers.

Finally, by introducing $\alpha_0^h = -\frac{\omega h_0}{V_\infty}$ and $\tilde{\alpha}^h = -\frac{\omega \dot{\tilde{h}}}{V_\infty}$, dimensional analysis leads to the following expression:

$$\tilde{C}_L = \frac{\tilde{L}}{P_{dyn}.B} = \frac{\partial \tilde{C}_L^{pitch}}{\partial \theta}.\tilde{\theta} + \frac{\partial \tilde{C}_L^{heave}}{\partial \alpha^h}.\tilde{\alpha}^h \qquad (6)$$

where,

$$\frac{\partial \tilde{C}_L^{pitch}}{\partial \theta}(k, \mathrm{Re}) = \frac{L_0^{pitch}.e^{i\varphi_L^p}}{\theta_0 P_{dyn}.B}$$

$$\frac{\partial \tilde{C}_L^{heave}}{\partial \alpha^h}(k,\mathrm{Re}) = \frac{L_0^{heave} e^{i\varphi_L^h}}{\alpha_0 P_{dyn}.B} \quad (7)$$

Note that for very slow dynamic (k<<1) the result should be in accordance with the potential theory. Then we should have for the derivative of the lift coefficient:

$$\left\| \frac{\partial C_L^{pitch}}{\partial \theta} \right\|, \left\| \frac{\partial C_L^{heave}}{\partial \alpha^h} \right\| \xrightarrow{k=0} 2\pi \quad (8)$$

$$\varphi_L^p, \varphi_L^h \xrightarrow{k=0} 0 \quad (9)$$

The phase of the pitch motion lift shall tend to 0 for slow motions (lift in phase with pitch):
It should be noted that the heave motion produces a lift for which will tend to be in phase with the heave induce angle α^h, therefore $\varphi_L^h \xrightarrow{k=0} 0$ leads to $-\pi/2$ of phase lag with the heave motion itself.
The unsteady effect will act on the amplitude and the phase lag of the lift response. It is important to note that any steady and unsteady effect (wake, added mass) can be modelled through this approach. It is therefore a practical way to compute a very complete hydrodynamic model for harmonic motions.
Following the same approach we get for the pitching moment:

$$\frac{\partial \tilde{C}_m^{pitch}}{\partial \theta}(k,\mathrm{Re}) = \frac{M_0^{pitch}.e^{i\varphi_m^p}}{\theta_0 P_{dyn}.B}$$

$$\frac{\partial \tilde{C}_m^{heave}}{\partial \alpha^h}(k,\mathrm{Re}) = \frac{M_0^{heave} e^{i\varphi_m^h}}{\alpha_0^h P_{dyn}.B} \quad (10)$$

2.1.2 2D CFD CALCULATIONS

The objective of the 2D CFD analysis is to compute the amplitude $L_0^{pitch}(k,\mathrm{Re})$ and the phase $\varphi_L^p(k,\mathrm{Re})$ (or the equivalent for the heaving motion) of the hydrodynamic response.
Each motion (pitch or heave) is imposed to a profile in a constant infinite flow defining a couple (*k*, *Re*). The unsteady calculation is run and the lift computed for each time step. Thus, the Fast Fourier Transformation of the resulting signal is achieved. Only the first harmonic is kept here assuming that it contains the major part of the response. This hypothesis is validated in §3.1.1.
To build the database, the profile shape from the 2006 Farr Yacht Design IMOCA 60 fin is used (see figure 4). Computations were carried out using the ISIS-CFD solver described in section §2.2.1. The 2D fluid domain of 51610 cells is 12 chord lengths and 10 chord heights. Far field conditions are used for all external boundaries, except the outlet where a constant pressure is imposed. A wall-function approach associated with the *k-*ω SST Menter turbulence model is used [9]. Grid and time step independency were checked before running the complete database.

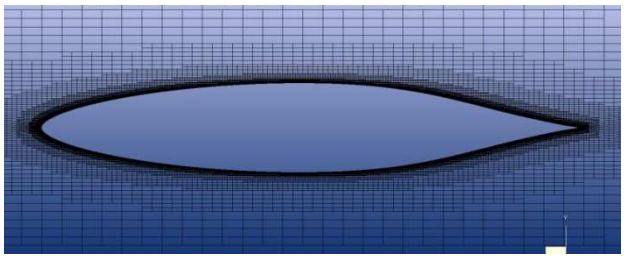

Figure 4 *Close view of the profile mesh*

2.1.2.3 COMPUTED UNSTEADY HYDRODYNAMIC MATRIX DATABASE

For a given appendage, the domain of interest for the hydrodynamic calculations in terms of reduced frequency and Reynolds number can be obtained by considering the range of speed of the boat and the range of chord. Calculations are run for a domain in Reynolds Number and reduced frequency that contains the actual reduced frequency (of the mode) calculated for each speed.
An example is given below.

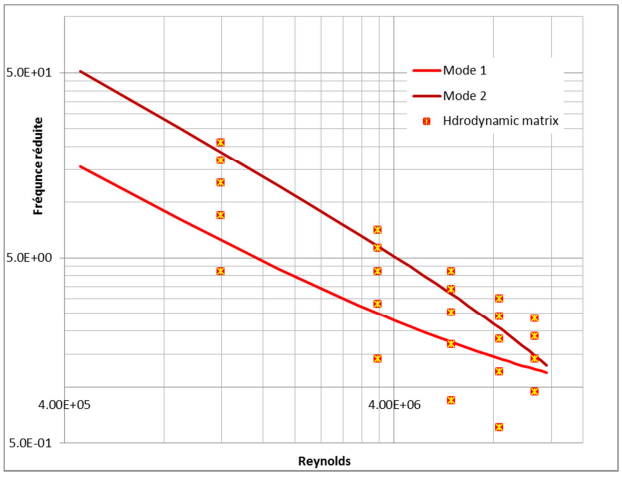

Figure 5 *Schematic flutter diagram and associated 2D CFD calculations points in Reynolds, Reduced frequency units*

2.1.3 THEODORSEN SOLUTION

The model of Theodorsen [6, 7] is derived from a theory of unsteady aerodynamics for a thin 2D airfoil undergoing small harmonic oscillations in incompressible and inviscid flow.
It contains added-mass and quasi-steady contributions as well as the effect of the wake, included in the Theodorsen's function *C(k)*, for both lift force and momentum. No information concerning the drag can be deduced from this model.
With the notations used in section 2.1 and figure 3, the expressions of lift and momentum (expressed at the centre of rotation) are given by Eq. (11).

$$L(t) = 2\pi\rho V_\infty bC(\tfrac{k}{2})\left[-\dot{h} + V_\infty\theta + b(\frac{1}{2} - a)\dot{\theta}\right] + \pi.\rho.b^2(-\ddot{h} + V_\infty.\dot{\theta} - b.a.\ddot{\theta})$$

$$M_O(t) = -\pi\rho b^3\left[-\tfrac{1}{2}\ddot{h} + V_\infty\dot{\theta} + b(\tfrac{1}{8} - \tfrac{a}{2})\ddot{\theta}\right] \quad (11)$$

with,

$$C(k) = \frac{H_1^{(2)}(k)}{H_1^{(2)}(k) + H_0^{(2)}(k)} \quad (12)$$

$H_n^{(2)}(k)$ being the n[th] Hankel function of second species

2.2 NAVIER-STOKES SOLVER

2.2.1 ISIS-CFD CODE

The ISIS-CFD code, developed by the METHRIC team of the LHEEA Lab. of Ecole Centrale Nantes, UMR-CNRS 6598, solves the incompressible Unsteady Reynolds- Averaged Navier-Stokes (URANS) equations in a strongly conservative way. It is based on a fully unstructured, cell-centered finite-volume method to build the spatial discretization of the conservation equations. Pressure-velocity coupling is obtained through a Rhie & Chow SIMPLE-type method: in each time step, the velocity update comes from the momentum equations and the pressure is given by the mass conservation, transformed into a pressure equation. The temporal discretisation scheme is the Backward Difference Formula of order 2 (BDF2) when dealing with unsteady configurations. For each time step, an inner loop (denoted by non-linear loop) associated to a Picard linearization is used to solve the non-linearities of the system and converge all the sequential coupled equations. In the case of turbulent flows, additional transport equations for modeled variables are solved in a form similar to the momentum equations and they can be discretized and solved using the same principles. An Arbitrary Lagrangian Eulerian (ALE) formulation is used to take into account modification of the fluid spatial domain due to body motion and deformation [10]. Free surface flow is addressed with an interface capturing method, by solving a conservation equation for the volume fraction of water, with specific compressive discretization schemes [8]. The code is fully parallel using the MPI (Message Passing Interface) protocol.

2.2.2 FSI COUPLING WITH MODAL APPROACH

The modal approach in the ISIS-CFD code uses the n first natural modes of vibration of the dry structure as input. Since the eigen modal matrix makes the mass matrix and stiffness matrix orthogonal, the temporal resolution of the structure is then reduced to an set of uncoupled degree of freedom (DOF) governed by the n modal equations given by Eq. (13).

$$\ddot{q}_i + 2\varepsilon_i\omega_i\dot{q}_i + \omega_i^2 q_i = \phi_i^T f(t) \quad i \in [1, n] \quad (13)$$

where ϕ_i is the i^{th} modal vector normalized by the mass, q_i the amplitude of the mode, $\omega_i = 2\pi f_i$ the pulsation, f_i the frequency, and ε_i is a possible damping coefficient assuming the Rayleigh damping hypothesis (damping matrix proportional to the mass and stiffness matrix). $f(t)$ refers to the fluid force acting on the structure. The total shape deformation is then given by Eq.(14).

$$\sum_{i=1}^{n} q_i(t)\phi_i(x) \quad (14)$$

These equations are fully coupled with the resolution of the fluid flow through an internal implicit coupling. At each non-linear iteration of the fluid solver (within the same time step), all the DOF of the structure are solved and updated. A Radial Basis Function (RBF) approach is used here to compute the source term of Eq.(13) and as a mesh deformation technique to recover a body-fitted mesh after each resolution of the structure.

3. RESULTS

3.1 SOME 2D RESULTS TO BUILD THE DATABASE

3.1.1 VERIFICATION OF THE HARMONIC CONTENT

Using the FFT, it was verified that all disregarded harmonics are less than 5% of amplitude of the fundamental mode.

3.1.2 VERIFICATION OF THE LINEARITY

The first step was to validate the assumption of linearity. Additive and multiplicative linearities were checked. This was performed for various reduced frequencies. Results are very good as shown in the example below.

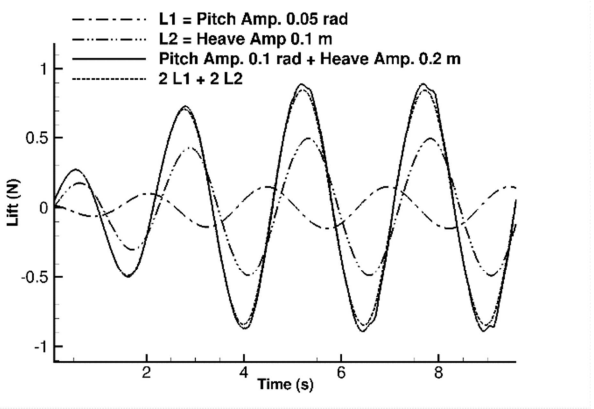

Figure 6 *Example of verification of lift force multiplicative, and additive linearity*

In figure 6 we observe good agreement between the hydrodynamic force generated by a combined motion, and the re-constructed force generated with separated

pitch and heave motions at medium to high dynamic motion (k=2.51 et Re=3.96e5).
The slight difference can be attributed to the amplitude of the motion which becomes larger with the combination of both pitch and heave associated with the factor 2 for the amplitude.

3.1.3 COMPARISON 2D CFD DATABASE VERSUS THEODORSEN

The results of 2D CFD are compared to the Theodorsen theory for lift and pitching moment in terms of module and phase.
The figures presented here show the results as a function of the reduced frequency and for all computed Reynolds Numbers. It seems that the Reynolds Number has a low influence on the results as it is not possible to differentiate the URANSE results at different Reynolds Number except for φ_m^p. However these results need to be consolidated as the database is incomplete as shown in figure 7.

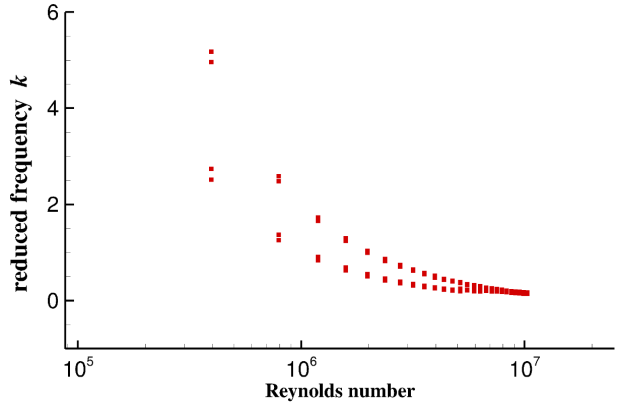

Figure 7 k versus Reynolds setting for the computed matrix

3.1.3.1 Lift

Comparisons for lift are given below. Even though $\frac{\partial C_L}{\partial \alpha_n};\frac{\partial C_L}{\partial \theta}$ are identical for the quasi-static regime, large differences appear for high dynamic regime.

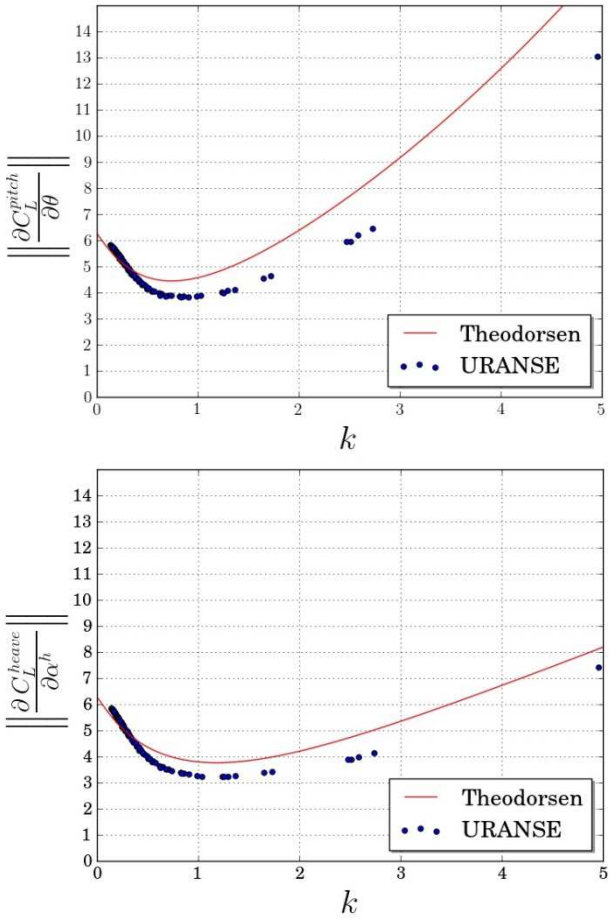

Figure 8*Module of the lift curve slope as a function of the reduced frequency*

The unsteady effect has a large impact on the lift curve coefficient as the minimum is more than 30% below quasi-static value, and for large value of k it increases continuously, (figure8).
We observe that both approaches follow very similar trends. For $k=0$ both curves tend to the potential lift curve slope coefficient 2π. It should be noted that the CFD calculation presents the actual foil profile and therefore tends to the actual value which is close but not equal to 2π.

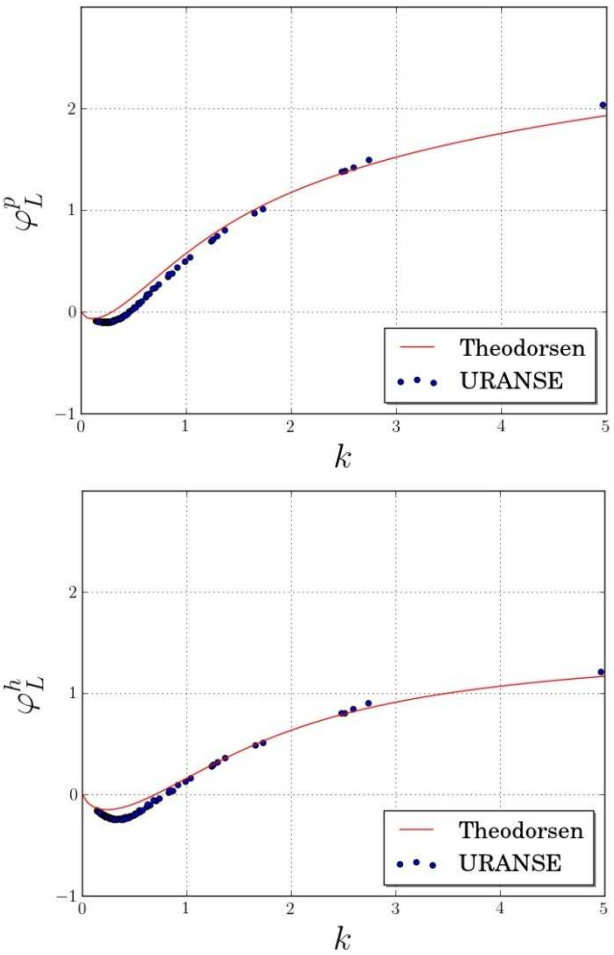

Figure 9 *Phase of the lift curve slope as a function of the reduced frequency (pitch left, heave right)*

Figure 9, the phases present a good agreement between the two methods. The phases are in line with the quasi-static, φ_L^p, φ_L tend to 0 for low values of *k*, which traduce no phase delay with $\tilde{\theta}$ the pitch motion, and $\tilde{\alpha}^h$ the heave induced angle.

3.1.3.2 Pitching moment

A good agreement can also be noticed between CFD and Theodorsen theory, (figure 10).

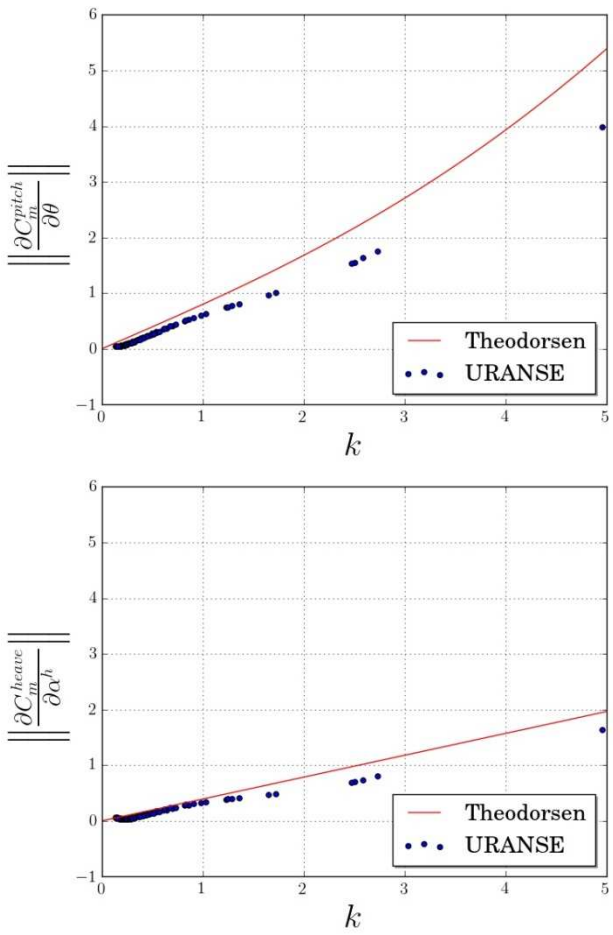

Figure 10 *Module of the lift curve slope as a function of the reduced frequency for heave motion (left), and pitch motion (right)*

Again the quasi-static value is matched as the pitching moments tend to zero on this profile where the rotation centre is defined at ¼*B* of the leading edge. This is verified for both pitch and heave.
Similar to the lift, the quasi-static pitching moment is not a proper model to define a configuration involving high dynamic phenomena.

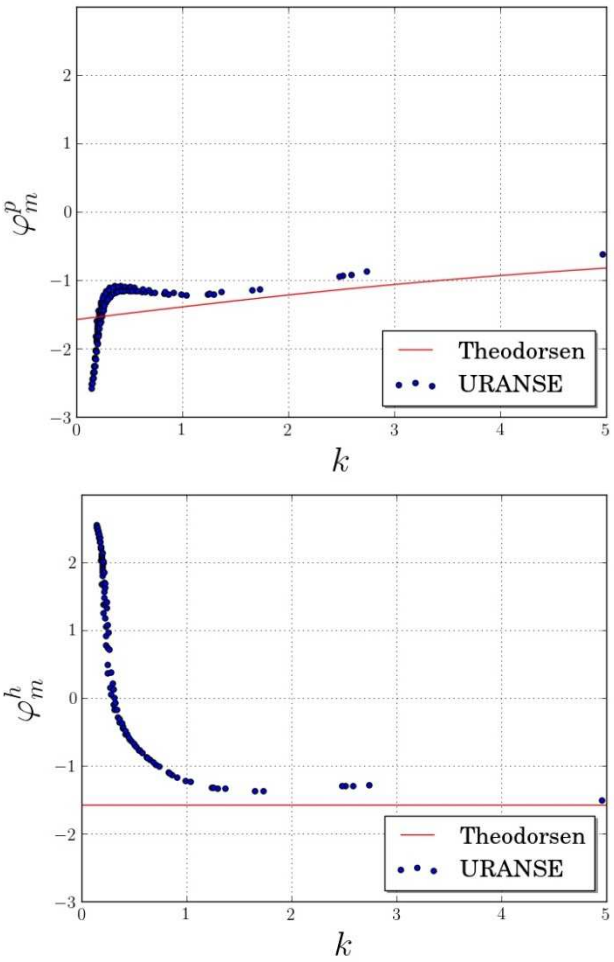

Figure 11 *Phase of the lift curve slope as a function of the reduced frequency for heave motion (left), and pitch motion (right)*

Concerning the phase, for large values of reduced frequency, the models agree fairly well. However, there are large differences at low frequencies. Even though the impact is probably limited as it happens as the amplitude tends to zero, the reason for these discrepancies is not known at this point. It may be related to the viscous friction that becomes more important than the pressure loads. Also the thickness of the profile may play a role since the Theodorsen model only considers a zero-thickness profile.
Also, for high values of *k* the presented results can be influenced by the lower Reynolds number used compared to the ones used for low values of *k*, see figure 7.

3.2 RESULTS WITH THE IMOCA 60 KEEL

The objective of this work is to enable the analysis of stiff, light lifting structures. However in order to validate the implementation of the models the case study used here is the FARR IMOCA 2006 keel that suffered the onset of flutter, and was successfully modelled in [1]. This keel presents low reduced frequencies, and is not a test for the hydrodynamic model but rather a test to check that once the fluid model is implemented, the results are in agreement with previously validated results.

3.2.1 FREQUENCY HYDRO-STRUCTURAL FLUTTER ANALYSIS (WITH DIFFERENT FLUID MODEL)

The linearized unsteady 2D hydrodynamic model of the lift force (not yet the pitching moment) was implemented in the flutter analysis tool. The database produced during this work was loaded in the software. During the computation, an interpolation between the calculated points is used to get the actual hydrodynamic forces for the couple (*k*, *Re*).
The 2006 Farr Yacht Design Imoca 60 keel was analysed and compared to the previous version of the model which considered quasi-static hydrodynamic with pitch and heave induced angles.

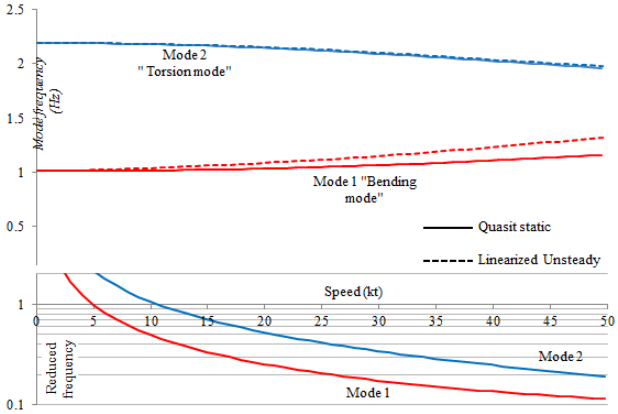

Figure 12 *Evolution of the natural frequencies of the keel as a function of speed (top), corresponding reduced frequencies*

Results are very consistent for this keel which presents low reduced frequencies as shown at the bottom of figure 12. As shown in figure 13, the slight differences do not significantly change the flutter speed (around 18 knots).

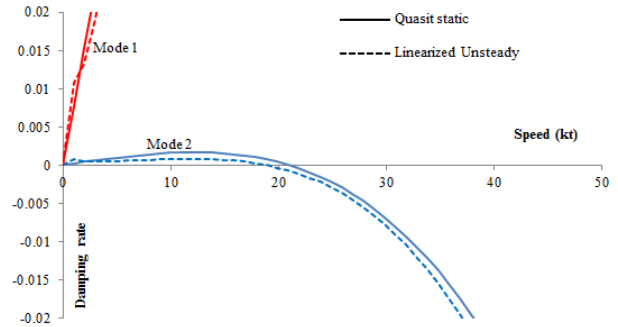

Figure 13 *Damping rate as a function of the boat speed, comparison between quasi-static and linearized unsteady hydrodynamic, (flutter speed is very close to 20 knots)*

As expected no significant differences are found on this keel. This is due to the low natural frequencies that induce an almost quasi-static hydrodynamic regime. Here the quasi-static model is sufficient to model correctly the physics of the flow.
It is different for a lighter structure, and the unsteady effects will have a larger influence. The method is now ready for this future step.

Next steps are to include pitching moment into the code, and to allow the definition of curved foils.

3.2.2 FSI COUPLED MODAL APPROACH WITH CFD

For this configuration, simulations have been done with a full hexaedron mesh of 3.8 million cells designed for a wall-function approach of the turbulence ($y+=30$).
Figure 14 and 15 show a global and a closer view of the mesh.
The time step is set at 0.01 s. The Reynolds stress tensor is computed using the k-ω (SST-Menter) model [9].

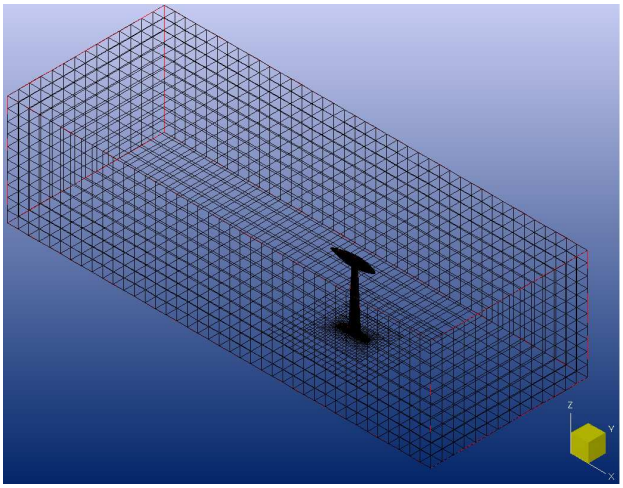

Figure 14 *CFD mesh generated for the IMOCA's keel, global view*

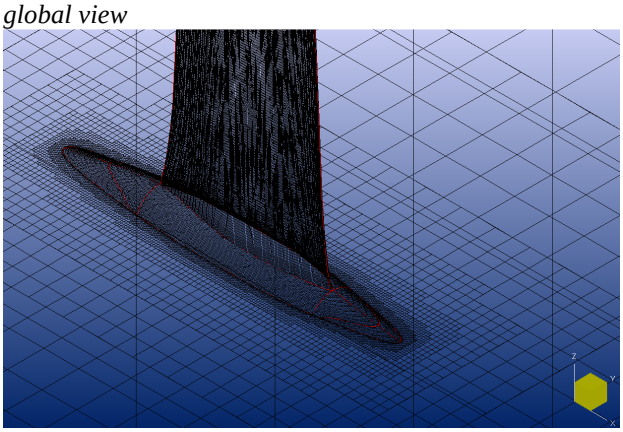

Figure 15 *CFD mesh generated for the IMOCA's keel feet*

Concerning the structural part, the information of two first modes used for the frequential hydro-elastic analysis was simply converted into an input data file formatted for the CFD code. At the beginning of the simulation, the flow is at rest. The body is sped up to reach its nominal forward velocity within a short time (1 s). FSI resolution is activated from the start. Perturbations generated during this violent transient state excite the structure modes. Thereafter, we can follow the evolution of their amplitudes in time.
Results show that the approach succeeds in catching the flutter occurrence for a velocity between 8 m/s and 9 m/s (figure 16).

For velocity of 8 m/s, it can be shown that the time derivative of the modal amplitude tends to slowly decrease, whereas at 9m/s, the flutter velocity is exceeded, which results in an increase of the modal amplitude velocity (and then an increase of the modal amplitude itself) in time.

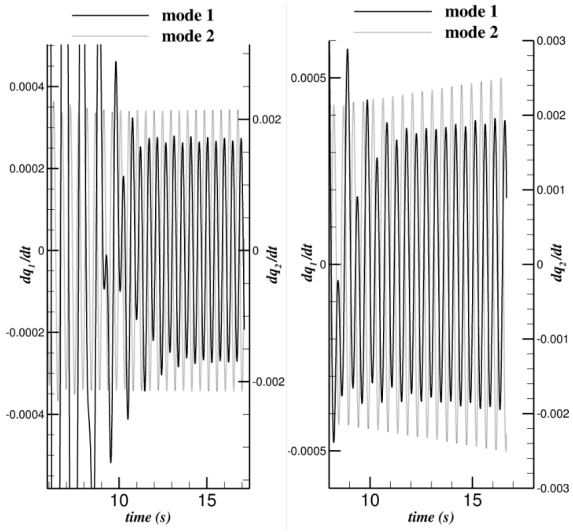

Figure 16 *time derivative of the modal amplitude, for a boat speed of 8 m/s (left) and 9 m/s (right)*

The range of the flutter velocity found here is a slightly lower than the value found by the hydro-elastic tool. However, additional simulations should be run to assess numerical convergence (grid, time step,...).
The fully coupled time marching approach between modal approach and RANSE solver is capable of detecting flutter phenomenon even if it requires large CPU time to accurately determine the range of the flutter velocity.

4. CONCLUSION

Two main approaches of flutter evaluation have been investigated in this on-going work. The first one corresponds to the frequency domain analysis which was developed by Bureau Veritas M&O. It requires a linearized 2D hydrodynamic model. The work presented in this paper uses CFD URANSE computations to set up a linearized unsteady hydrodynamic model. The linearity of the model requires verification, and is only valid for small motions around the equilibrium position. However, it can include unsteady effects, such as phase delay, amplitude modifications, and added mass in a very simple linear approach. The comparison with Theodorsen's theory allows good confidence in the results. The presented database is sparse, and further work is required. However, the method allows the use of the frequency flutter analysis tool for foils with high dynamic regime even if only driven by the Theodorsen model.
The modal approach that is fully coupled with CFD, contains fewer assumptions and captures more of the physics, such as 3D effects.
This approach requires running several unsteady simulations at different speeds via a dichotomic search to

determine the critical flutter velocity range. More accurate estimations of the flutter phenomenon can be expected, at the expense of far larger computational power.
The tools are complementary; the frequency analysis is able to investigate a large number of designs in a limited amount of time, and the FSI computation can provide a precise verification including a broader range of physical phenomenon.

ACKNOWLEDGEMENTS

This work was granted access to the HPC resources of CINES and IDRIS under the allocation 2B0129 made by GENCI (Grand Equipement National de Calcul Intensif).

REFERENCES

1. L. Mouton, A. Finkelstein "Exploratory study on the flutter behavior of modern yacht keels and appendages3, *High performance Yacht Design, Auckland, 2015.*
2. I.H. Abbott, A.E. Von Doenhoff , "Theory Of Wing Sections", *Dover*, 1958
3. R. Balze, H. Devaux, "Flutter of racing yacht keels and appendages", *Innovation in High Performance Sailing Yachts INNOVSAIL, Lorient*, 2013 .
4. O. M. Faltinsen, "Hydrodynamics of High-Speed Marine Vehicles", *2006, Cambridge*
5. R. D. Blevins, "Flow-induced vibration", *Van Nostrand Reinhold Company*
6. T. Theodorsen, "General theory of aerodynamic instability and the mechanism of flutter", *NACA Report 496, 1979*
7. H. Hodges Dewey and G. Alvin, "Introduction to structural dynamics and aeroelasticity", *Cambridge University Press 15, 2002*
8. P. Queutey, and M. Visonneau,, "An interface capturing method for free-surface hydrodynamic flows", *Computers & fluids 9, 2007*
9. F.R. Menter, "Two-equation eddy-viscosity turbulence models for engineering applications", *AIAA journal, 1994*
10. L. Leroyer, S. Barré, J.M. Kobus and M. Visonneau, "Experimental and numerical investigations of the flow around an oar blade", *Journal of Marine Science and Technology 13*, 2008

AUTHORS BIOGRAPHY

A. Leroyer holds the current position of Associate Professor at the LHEEA lab. of Centrale Nantes since 2005. His research topics in the METHRIC group are mainly focused on the methodologies to integrate new physical phenomena inside a Navier-Stokes solver, as the fluid-structure interaction and the numerical modelling of cavitation. He is part of the developer team of the ISIS-CFD code.

L. Mouton holds the current position of structural engineer in the composite department of Bureau Veritas Marine & Offshore. He works for research and developments on marine composite structure and bonding.

G.B. Deng holds a research position in the METHRIC group of LHEEA at Centrale Nantes, France. His main activities concern CFD code development and application for hydrodynamics. His recent activities concern overset development.

P. Queutey entered CNRS as Research Scientist in 1990. Head of the METHRIC team of the LHEEA Lab. since 2012, his main research themes are in the context of Computational Fluid Dynamics (CFD) with the development of numerical schemes for viscous incompressible flows with specific treatment of interface capturing method suitable for sharp prediction of free-surface flows with application to fully unstructured grids for complex geometries. He contributes to the development of the in-house ISIS-CFD of the team.

T. Soler completed his master in Hydrodynamics at Centrale Nantes in 2016. His master thesis was focused on the work proposed in this article.

A. Finkelstein holds a position of senior designer engineer. Alon joined Farr Design in January 2003 and is responsible for research and design of appendages.